ACS SENSORS

pubs.acs.org/acssensors

Article

Voltammetric Selectivity in Detection of Ionized Perfluoroalkyl Substances at Micro-Interfaces between Immiscible Electrolyte Solutions

Gazi Jahirul Islam and Damien W. M. Arrigan*

Cite This: *ACS Sens.* 2022, 7, 2960−2967

Read Online

ACCESS | Metrics & More | Article Recommendations | Supporting Information

ABSTRACT: Widespread contamination by per- and polyfluoroalkyl substances (PFAS) and concern about their health impacts require the availability of rapid sensing approaches. In this research, four PFAS, perfluorooctanoic acid (PFOA), perfluorobutanesulfonic acid (PFBS), perfluorohexanesulfonic acid (PFHxS), and perfluorooctanesulfonic acid (PFOS), were studied at micropipette-based interfaces between two immiscible electrolyte solutions (μITIES) to assess the potentiality for their detection by ion transfer voltammetry. All four PFAS substances were detected by ion transfer voltammetry at the μITIES, with half-wave transfer potentials ($E_{1/2}$ vs Ag/AgCl) for PFOS, PFHxS, PFBS, and PFOA of 0.34, 0.32, 0.25, and 0.23 V, respectively. The selectivity of the μITIES for detection of PFAS mixtures was investigated. Among the six combinations of the four compounds, most combinations were detectable, except PFOA + PFBS and PFHxS + PFOS, because of unresolved ion transfer voltammograms. These findings provide a basis for the design of new PFAS sensing strategies based on ion transfer voltammetry.

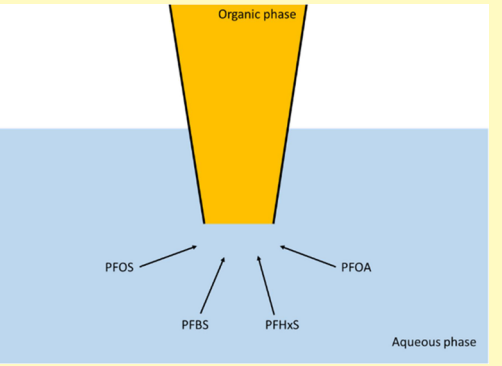

KEYWORDS: *PFAS, micropipette, ion transfer voltammetry, liquid−liquid interface, μITIES*

Per- and polyfluoroalkyl substances (PFAS) are a group of synthetic chemicals consisting of fluoroalkyl chains from 4 to 18 carbon atoms in length, with all or almost all hydrogen atoms substituted with fluorine atoms and with a carboxylic acid, sulfonate, or alcohol at the end of the chain.[1,2] Because of the strength of the C−F bond, these compounds are remarkably stable and have found numerous applications in industrial and domestic settings, for example, fire-fighting foams, metal plating baths, lubricants, paints, polishes, food packaging, aerospace, automotive, construction, electronics, and military.[3−8] PFAS are of globally emerging concern because of their high environmental persistence with long biological half-lives, toxicity,[9,10] and high levels of accumulation in plants and animals[11,12] that are linked to various health conditions such as immunosuppression, cancer, liver damage, and hormone disruption.[13−16]

A variety of analytical methods are available for the determination of PFAS. For example, gas chromatography−mass spectrometry (GC−MS),[17,18] high-performance liquid chromatography−mass spectrometry (HPLC-MS),[19,20] liquid chromatography−tandem mass spectrometry (LC−MS−MS),[21,22] colorimetric detection,[23,24] and fluorimetric analysis[25] are used for ultratrace analysis. Although these methods have achieved excellent performances, their disadvantages include use of complex and sophisticated instrumentation with high costs for establishment and maintenance, requirement for extensive sample pretreatment, time consumption, and need for highly trained personnel. More importantly, these are rarely suited for in-field applications.[26] Sensor approaches based on electrochemistry or other transduction strategies offer ways to overcome those difficulties while maintaining suitable analytical performances.

A variety of electrochemical sensing strategies for PFAS have been reported recently. One such approach is the combination of electrochemical sensing with molecularly imprinted polymers (MIPs), which are a popular target-recognition strategy for specific detection and are suitable for use in a range of conditions.[27,28] MIP-based electrochemical sensors for redox-inactive PFAS detection have been reported.[29,30] Karimian et al.[30] developed a sensor for perfluorooctane sulfonate (PFOS) based on an electrode modified with a MIP film of *o*-phenylenediamine (o-PD) and achieved a limit of detection (LOD) of 0.04 nM. Recently, Lu et al.[31] presented an ultrasensitive voltammetric sensor for PFOS detection

Received: May 22, 2022
Accepted: August 29, 2022
Published: September 16, 2022

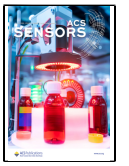

based on an electrode modified with a thin coating of gold nanostars and a MIP, achieving a LOD of 0.02 nM. Dick and co-workers[32] developed a o-PD MIP-modified electrode to detect PFOS, with a LOD of 0.05 nM. This group also reported a MIP-modified microelectrode for the detection of ammonium perfluoro(2-methyl-3-oxahexanoate) (GenX), with excellent selectivity in the presence of humic acid, chloride, and PFOS.[33] Because of the redox-inactive nature of most PFAS, MIP-based electrochemical sensors employ an in-solution redox-active signaling species. Clark and Dick[34,35] showed that ambient oxygen in a sample can be used for this purpose.

Because of the chemical stability of PFAS, their direct detection by electrochemical oxidation or reduction is not feasible for sensing purposes. This limitation can be overcome by employing electrochemistry at the interface between two immiscible electrolyte solutions (ITIES),[36−39] which employs the transfer of ionized species across the interface to produce the electrochemical signal. Ion transfer electrochemistry of PFAS was investigated by Amemiya and co-workers[40] to quantify the lipophilicity of perfluoroalkyl chains. They used this approach to measure the partition coefficients of perfluoroalkyl carboxylates and sulfonates at *n*-octanol/water interfaces to characterize the lipophilicities of perfluoroalkyl and alkyl oxoanions with the same chain length. Amemiya's group[41] also reported on PFAS detection by ion transfer stripping voltammetry at the ITIES formed between an aqueous electrolyte and a plasticized polymeric thin film on an electrode, achieving a LOD of 50 pM for PFOS, following a 30 min preconcentration period. Recently, Viada et al.[42] reported on PFOS detection by ion transfer differential pulse stripping voltammetry (DPSV) at an array of μITIES. The LOD for PFOS in an aqueous electrolyte was 30 pM (i.e., 0.015 μg L^{-1}) following a 5 min preconcentration period. Viada et al.[42] also studied sample matrix effects, finding changes in sensitivity and LOD relative to those in pure aqueous electrolyte solutions.

The advantage of ion transfer voltammetry at the ITIES is that detection is based on the properties of the ionized analyte, removing the requirement for use of a redox-label or indicator. Given the recent achievement of picomolar LODs and assessment of matrix effects for PFOS, the present study is focused on characterizing selectivity related to sensing of mixtures of PFAS by ion transfer voltammetry, so as to understand whether this approach might be useful for detection of PFAS mixtures. In particular, this study focused on the ion transfer electrochemistry of four PFAS, perfluorooctanoic acid (PFOA), perfluorobutanesulfonic acid (PFBS), perfluorohexanesulfonic acid (PFHxS), and PFOS, at μITIES formed at the tips of micropipettes. The four chosen PFAS have very close carbon atom numbers to better gauge their impact on detection in mixtures. The major objective of this investigation was to evaluate the inherent selectivity of the μITIES for the detection of PFAS substances in their mixtures.

EXPERIMENTAL SECTION

Reagents. All the reagents were purchased from Sigma-Aldrich Australia Ltd. and used as received unless indicated otherwise. The organic electrolyte bis(triphenylphosphoranylidene)ammonium tetrakis(4-chlorophenyl)borate (BTPPATPBCl) was prepared by metathesis of equimolar amounts of bis(triphenylphosphoranylidene)-ammonium chloride (BTPPACl) and potassium tetrakis(4-chlorophenyl)borate (KTPBCl).[43] BTPPATPBCl (0.01 M) solutions were prepared in 1,2-dichloroethane (DCE). Chlorotrimethylsilane was used for silanization of pipettes. Aqueous solutions were prepared in purified water from a USF Purelab plus UV (resistivity: 18.2 MΩ cm). Pentadecafluorooctanoic acid, 98% (PFOA) and perfluorooctanesulfonic acid, potassium salt, 97% (PFOS) were purchased from STREM Chemicals. Perfluorobutanesulfonic acid (PFBS) and perfluorohexanesulfonic acid (PFHxS) were purchased from Sigma-Aldrich Australia Ltd.

Fabrication of Micropipettes. Micropipettes were prepared from borosilicate capillaries (O.D. 1.0 mm; I.D. 0.75 mm) using a P2000 laser pipette puller (Sutter Instruments) using five programmable parameters heat (260), filament (3), velocity (15), delay (200), and pull (170). Before pulling, the capillaries were rinsed with water and acetone and sonicated in a 50:50 water−methanol mixture for 10 min. After drying, the capillaries were pulled by the pipette puller. Then, the inner surfaces of the pipettes were silanized with chlorotrimethylsilane in a simple vaporization process. The pipettes were placed upturned (i.e., pulled tips pointing upward and away from the vessel) in holes in the lid of a sealed vessel containing a drop of chlorotrimethylsilane. As chlorotrimethylsilane vaporized at room temperature, the vapor passed through the pipettes so that the inner walls were silanized. This was allowed to take place for ca. 30 min, and then, the pipettes were removed from the vessel and allowed to stand in air for 3−5 h. Pipette tips were gently abraded on a clean surface, visually inspected using an optical microscope, then characterized by ion-transfer cyclic voltammetry (Figure S1). Stable ion-transfer cyclic voltammograms indicated a pipette suitable for experiments. Pipette radii were determined from the steady-state current for the transfer of tetraethylammonium ions from the outer (aqueous) solution to the inner (DCE) solution (Figure S1 and Table S1).

Electrochemical Measurements. Electrochemical measurements were conducted using an Autolab PGSTAT302N without a low current module (Metrohm Autolab, Utrecht, The Netherlands) with NOVA software. The organic phase electrolyte was introduced inside the pipette, and the organic reference solution was placed on the top of the organic phase. Then, the pipette was immersed into the aqueous phase in a small beaker so that the ITIES formed at the tip of the pipette. The pipette was held in a slot cut in a rubber stopper which was held in place by a laboratory clamp stand. A two-electrode cell was employed for all experiments, using Ag/AgCl electrodes on each side of the ITIES as combined reference/counter electrodes. All potentials are reported versus the experimentally used Ag/AgCl electrodes. Cyclic voltammetry (CV) was employed at 10 mV s^{-1} in all cases: forward scans were from higher potential to lower potential and reverse scans from lower potential to higher potential, corresponding to anion transfer from the aqueous (outer) phase to the organic (inner) phase on the forward scan and the reverse transfer process on the reverse scan. Differential pulse voltammetry (DPV) was carried out in reverse scan mode, from 0.1 to 0.6 V. The DPV conditioning potential, equilibrium time, step potential, modulation amplitude, modulation time, and interval time were 0.1 V, 30 s, 0.005 V, 0.05 V, 0.04 s, and 0.5 s, respectively. Initially, a blank voltammogram (without analyte) was run, and then, the analyte was spiked from a stock solution into the aqueous phase. Background subtraction was applied unless indicated otherwise. Plots of current versus concentration use data based on averages of three measurements with error bars of ±1 standard deviation; where error bars are not visible, they are smaller than the symbol sized used in the graph. Under the conditions employed, stable voltammetry was obtained at higher concentrations; without silanization, unstable voltammograms were recorded. Pipettes showing unstable voltammograms were not used for further experiments. Scheme 1 displays the electrochemical cell composition.

Scheme 1. Electrochemical Cell Composition Employed in Studies of PFAS Ion Transfer Voltammetry

Ag	AgCl	Sat'd BTPPACl in 10 mM LiCl	10 mM BTPPATPBCl in DCE	x μM PFAS in 10 mM LiCl	AgCl	Ag

https://doi.org/10.1021/acssensors.2c01100
ACS Sens. 2022, 7, 2960−2967

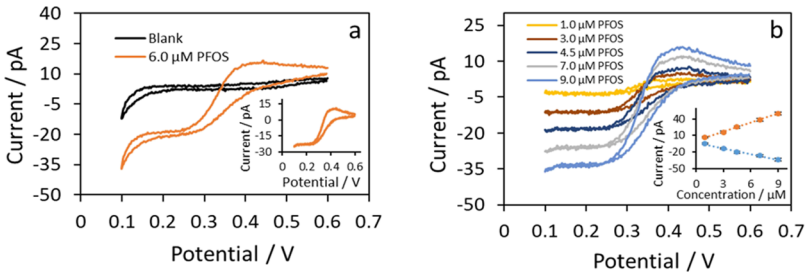

Figure 1. (a) CV of 6.0 μM PFOS and of blank; inset is the background-subtracted CV. (b) background subtracted CVs of 1.0, 3.0, 4.5, 7.0, and 9.0 μM PFOS; inset is the current vs concentration plot for both forward and reverse scan currents. Pipette radius: 8.5 μm.

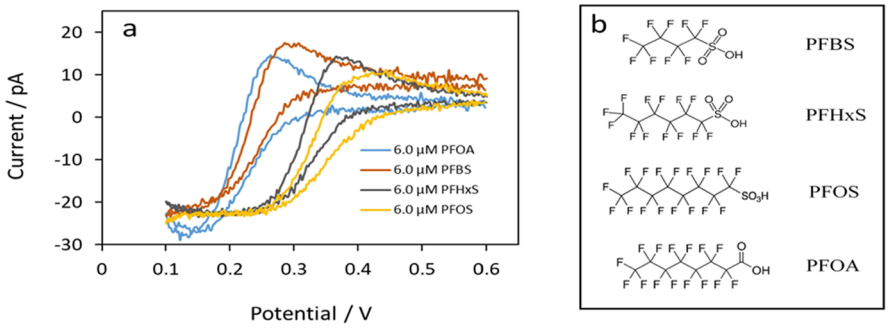

Figure 2. (a) Background-subtracted CV of 6 μM PFOA, 6 μM PFBS, 6 μM PFHxS and 6 μM PFOS at 8.4, 7.9, 7.9 and 8.5 μm radii μITIES, respectively. Other conditions as noted in Scheme 1. (b) Structures of the respective PFAS substances.

Table 1. Data Obtained from Ion-Transfer Voltammetry at a μITIES for PFOS, PFHxS, PFBS, and PFOA

				LOD (μM)	
substance	$E_{1/2}$ from CV (V vs Ag/AgCl)	E_p from DPV (V vs Ag/AgCl)	D (cm^2 s^{-1})	CV	DPV
PFOS	0.34	0.32	4.5×10^{-6}	1.1	0.04
PFHxS	0.32	0.31	4.8×10^{-6}	0.7	0.02
PFBS	0.25	0.25	5.7×10^{-6}	0.2	0.03
PFOA	0.23	0.22	4.7×10^{-6}	0.6	0.05

RESULTS AND DISCUSSION

Cyclic Voltammetry. The transfer of perfluoroalkanesulfonates (PFOS, PFHxS, and PFBS) and perfluoroalkanecarboxylate (PFOA) across the μITIES was studied by CV to analyze their electrochemical behaviors. All PFAS were added to the aqueous phase of LiCl which had a natural pH of ca. 6. As the four PFAS were employed as either salts or acids, at this pH, all were ionized (based on published pK_a data[44,45]) and anionic, with a charge (z) of −1. All analytes produced well-defined CVs without indications of adsorption, emulsification, or instability of the interface. Figure 1a shows the CV of PFOS and its corresponding blank (i.e., in the absence of PFOS). On the forward scan (scanning from higher to lower potentials) a sigmoidal voltammetric wave was recorded, corresponding to transfer of the analyte from the aqueous phase to the organic phase inside the pipette under radial diffusion control.[46] On the other hand, the broad peak on the reverse scan (scanning from lower to higher potentials) indicates linear diffusion control of PFOS transfer from the inner organic phase to the aqueous phase.[46] These findings are in agreement with previous accounts of ion-transfer voltammetry of PFAS at the 1-octanol/water interface,[40] at the water/plasticized polymer membrane interface,[41] and of PFOS at a water/DCE μITIES array.[42]

The half-wave potential $E_{1/2}$ provides a qualitative property for an analyte within a particular supporting electrolyte solution. Figure 1a (inset) shows that in the forward scan for background-subtracted 6 μM PFOS, the ion transfer starts at 0.44 V and reaches the plateau at 0.24 V, and the $E_{1/2}$ is 0.34 V (see Figure S2 for estimation of $E_{1/2}$ values, being the potential at which the current is one half of the limiting current). For the reverse scan, PFOS transfer back to the aqueous phase gives a peak at 0.42 V. The background-subtracted voltammograms of PFOS in the concentration range 1−9 μM are shown in Figure 1b. The steady-state forward current (i_f) and backward or reverse peak current (i_b) for each concentration was measured and plotted versus the aqueous phase PFOS concentration (Figure 1b inset). The linear behavior is as expected for the modified Saito equation[47] and the Randles−Sevcik equation[48,49] for radial and linear diffusion-controlled currents, respectively. Similar electrochemical behavior was seen for PFHxS, PFBS, and PFOA (Figure 2a) with different transfer potentials according to their structures; the observed $E_{1/2}$ values are shown in Table 1. Diffusion coefficients (D) of the four PFAS were determined using the equation[50] (eq 1).

$$I_{ss} = 3.35\pi|z|FDCr \quad (1)$$

where I_{ss} is the steady state current, D, C, and z are the diffusion coefficient, concentration, and ionized charge of the transferring analyte; F and r are the Faraday constant and radius of the pipette used to form the interface, respectively. The value of z used for these experiments was −1. Equation 1,

https://doi.org/10.1021/acssensors.2c01100
ACS Sens. 2022, 7, 2960−2967

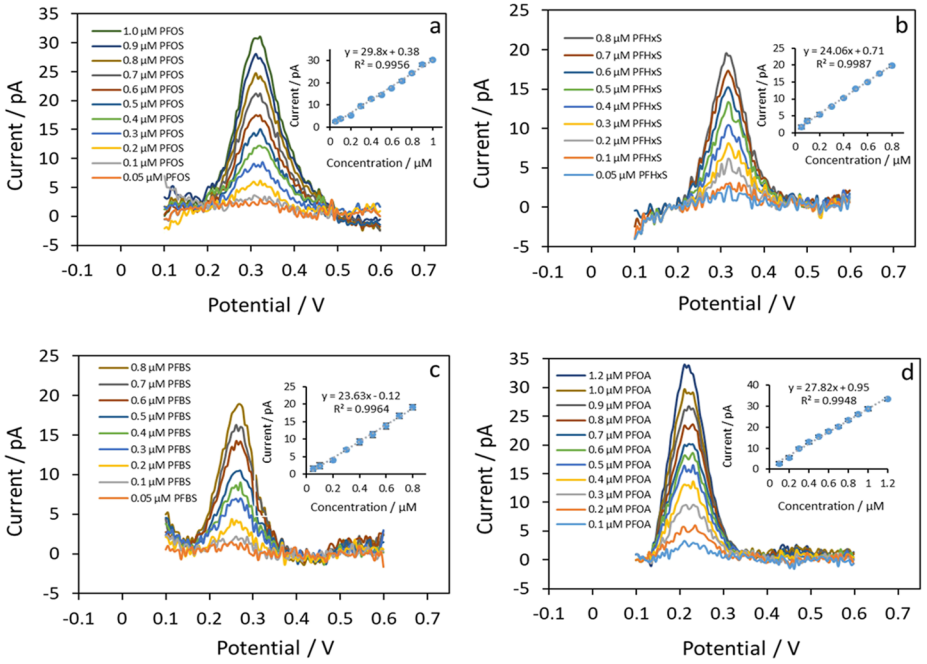

Figure 3. Background-subtracted DPV at different concentrations and the respective current vs concentration plots for (a) PFOS, (b) PFHxS, (c) PFBS, and (d) PFOA, at 8.5, 7.9, 7.9, and 8.4 μm radius μITIES, respectively. Other conditions are as shown in Scheme 1.

developed by Beattie et al.,[50] is an empirical equation developed for micrometer-scale pipettes that describes the steady-state current for ion transfer from the outer solution to the inner (filling) solution. Calculated diffusion coefficients of PFOS, PFHxS, PFBS, and PFOA in the aqueous phase are shown in Table 1 and are in good agreement with literature values (5.4×10^{-6}, 4.5×10^{-6}, 11×10^{-6}, and 4.9×10^{-6} cm^2 s^{-1}, respectively).[51]

Irrespective of the diffusion mode, the currents are concentration-dependent (Figure 1b inset). Although the purpose of this investigation was not trace analysis of PFAS, the LODs were estimated from the slopes of the calibration curves for the forward scans of the CVs using the formula LOD = $(3{\cdot}\sigma)/S$,[42] (S is the slope and σ is the y-intercept standard deviation of the linear regression line). The LODs of PFOS, PFHxS, PFBS, and PFOA (Table 1) indicate that low and sub-micromolar concentrations can be determined with this approach, although these levels are unsuitable for practical applications.

Comparison of the CVs of PFOS, PFHxS, PFBS, and PFOA. Figure 2 shows background-subtracted CVs for each of the PFAS analytes studied in this work. The voltammograms and the $E_{1/2}$ values (Table 1) indicate that the transfer potential of each species decreases with decreasing carbon number for the perfluoroalkanesulfonates. The CV forward scans for PFOS (8 carbon chain), PFHxS (6 carbon chain), and PFBS (4 carbon chain) show that the ion-transfer $E_{1/2}$ trends from 0.34 to 0.32 to 0.25 V, indicating a greater energy requirement to transfer each species.

The same pattern is seen with the reverse peak potential, at 0.42, 0.37, and 0.30 V, respectively. The forward scan starts from higher potential to lower potential. Therefore, the right hand side of the potential scale indicates lower energy of transfer and the left hand side of the potential scale indicates higher energy of transfer. The voltammograms indicated the order PFOS < PFHxS < PFBS in terms of the required energy to transfer, although the shapes of the voltammograms are all similar. This order of transfer corresponds to the reversed order of lipophilicity, which confirms that with a longer chain, PFOS is more lipophilic than those with a shorter chain. A similar result was found by Amemiya and co-workers,[41] who also compared PFOS transfer with octanesulfonate (OS^-) transfer. They found that the alkanesulfonate with the same chain length was less lipophilic than PFOS,[41] attributed to the electron-withdrawing effects of fluorine, which reduces the electron density and hydration of the sulfonate group.[40]

In contrast, PFOA was found to be less lipophilic than PFOS (Figure 2a). Although the carbon number of the fluorocarbon chains in PFOA and PFOS are the same (Figure 2b), transfer of PFOA required more energy, even more than PFBS. The estimated $E_{1/2}$ of PFOA is 0.23 V. The lower lipophilicity of perfluoroalkanecarboxylates is attributed to the greater hydration energy of the carboxylate group, which is smaller and more basic than the sulfonate group.[52]

CVs of a PFOA and PFOS mixture were studied to evaluate the capability for their detection in a mixture. The CV of the mixture (Figure S3) shows that it is not possible to detect them separately, despite the difference in their ion transfer $E_{1/2}$ values, which was the largest among the four PFAS studied. Based on these results, it is not be possible to distinguish them from CVs of their mixtures.

Differential Pulse Voltammetry. The detection of perfluoroalkanesulfonates and perfluoroalkanecarboxylates was achievable by CV at the micropipette-based μITIES. However, in mixtures, CV was unable to resolve their responses. The peak-shaped responses of DPV offer scope for improvement in mixture resolution. DPV at the pipette-based μITIES gave well-defined and sharper peaks at lower concentrations than possible by CV. Figure 3 shows the voltammograms and calibration curves obtained for PFOS, PFHxS, PFBS, and PFOA at a range of concentrations. The fluctuations in these voltammograms is attributed to noise at the low current ranges employed here. The lowest concentration detected using background-subtracted DPV for PFOS,

https://doi.org/10.1021/acssensors.2c01100
ACS Sens. 2022, 7, 2960−2967

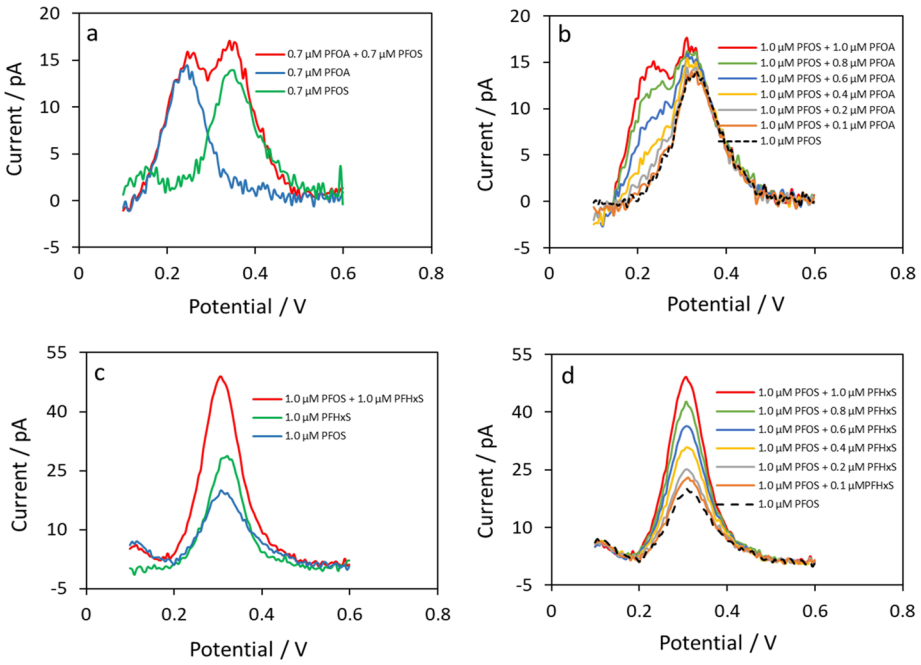

Figure 4. Background subtracted DPV of (a) 0.7 μM PFOA, 0.7 μM PFOS, and a mixture of 0.7 μM PFOA + 0.7 μM PFOS, (b) 0.1, 0.2, 0.4, 0.6, 0.8, and 1.0 μM PFOA with fixed 1.0 μM PFOS, (c) 1.0 μM PFHxS, 1.0 μM PFOS, and mixture of 1.0 μM PFHxS + 1.0 μM PFOS and (d) 0.1, 0.2, 0.4, 0.6, 0.8, and 1.0 μM PFHxS with fixed 1.0 μM PFOS. Pipette radius for (a) and (b) was 8.5 μm and for (c) and (d) was 7.9 μm. Other conditions are as noted in Scheme 1.

PFHxS, and PFBS was 0.05 μM; for PFOA, it was 0.1 μM. Linear current−concentration responses were obtained in all cases (insets, Figure 3).

Linear regression analyses of the DPV peak currents versus PFAS concentration were undertaken (Table S2) and the calculated LODs obtained (Table 1), which were approximately an order of magnitude lower than those from CV measurements (Table 1). The DPV peak potentials (E_p) for these four substances (Table 1) are in agreement with the $E_{1/2}$ values from the CV experiments. Peak widths at half height ($W_{1/2}$) of the DPV peaks were also determined (Table S2) and were slightly greater than those for a reversible process ($W_{1/2}$ 90.4 mV (z = 1)[53]).

DPV of Combinations of PFOA, PFBS, PFHxS, and PFOS. Mixtures of the four PFAS in six different combinations were studied by DPV. The aim of this study was to observe the impact on detection and analytical behavior of these mixtures and to understand which mixture combinations are practically detectable with this ion transfer voltammetry approach. At first, the mixture of PFOA and PFOS was analyzed. Figure 4a shows the individual voltammograms for 0.7 μM PFOA and 0.7 μM PFOS. These regular peak shapes overlap near the peak half-heights. On the other hand, the voltammogram of the mixture of 0.7 μM PFOA and 0.7 μM of PFOS gives a broad peak encompassing the two separate peaks but does still give two distinct peaks, confirming that two different species are present (Figure 4a). In the mixture, the peaks do not shift, but their currents are not exactly the same as obtained in the individual PFOA and PFOS responses at this concentration. The currents at different potentials for 0.7 μM PFOA and 0.7 μM PFOS and the current for the mixture of PFOA and PFOS are similar.

Figure 4b shows the voltammograms of 1.0 μM PFOS plus increasing concentrations of PFOA from 0 to 1.0 μM. The voltammograms clearly show that when the concentration difference between the two substances is high, the DPV does not provide an indication that two separate species are present in solution. At concentrations of PFOA from 0.4 μM and upward, a shoulder is present at the expected potential for PFOA and this increases in magnitude up to 1.0 μM PFOA at which point two separate peaks are seen in the voltammogram, as seen previously for the mixture of 0.7 μM PFOA and 0.7 μM PFOS. As a result, it can be determined that for detection of both PFOS and PFOA, their concentration ratio should not be more than 2:5. Similar findings were observed for the mixtures of PFOA + PFHxS, PFHxS + PFBS, and PFOS + PFBS (Figure S4). The detection of PFAS substances in these binary mixtures was possible for concentration ratios of 2:5.

Mixtures of PFOS + PFHxS and PFOA + PFBS, in which the transfer potentials were very close, were also analyzed. From Figure 4c, the individual voltammograms of 1.0 μM PFOS and 1.0 μM PFHxS are clear. However, because their transfer potentials are very close, they completely overlap each other. One the other hand, their equimolar (1.0 μM) mixture gives a single sharp peak like that for a single substance, and the peak area is nearly the same as the sum of the two individual peak areas. The sum of the peak currents of the individual PFOS and PFHxS at 0.24 V is nearly equal to the mixture peak current at that potential. Figure 4d shows the voltammograms for increasing concentrations of PFHxS, from 0 to 1.0 μM, with constant PFOS concentration at 1.0 μM. In this case, the current increased with the concentration PFHxS as if one type of species was present. Therefore, for this mixture, it is not possible to detect both components in the solution by this approach. Similar observations were seen for the mixture of PFBS + PFOA (Figure S4).

Figure 5 shows the DPV results for a mixture of the four PFAS studied here as well as individual voltammograms. The mixture of 1.0 μM of each of PFOA, PFBS, PFHxS, and PFOS produces a broad peak. The area of this peak is equal to the sum of the individual peak areas for PFOA, PFBS, PFHxS, and

https://doi.org/10.1021/acssensors.2c01100
ACS Sens. 2022, 7, 2960−2967

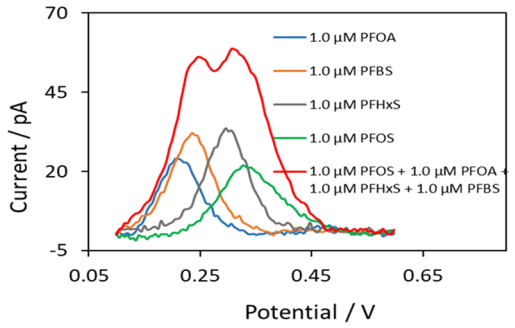

Figure 5. Background-subtracted DPVs of 1.0 μM PFOA, 1.0 μM PFBS, 1.0 μM PFHxS, 1.0 μM PFOS, and a mixture of 1.0 μM PFOA + 1.0 μM PFBS + 1.0 μM PFHxS + 1.0 μM PFOS. Pipette radii for PFOA, PFBS, PFHxS, and PFOS and mixture experiments are 8.4, 7.9, 7.9, 8.5, and 8.5 μm, respectively. Other conditions are as noted in Scheme 1.

PFOS. From this figure, it is clear that although there are four different substances present in the mixture, the voltammogram gives a signal like for two substances. Therefore, this is a limitation that if there is more than two PFAS present in the solution, their presence cannot be confirmed by DPV if their transfer potentials are very close together. Table 2 summarizes which mixture of two substances in solution are detectable or not by DPV at the μITIES.

Table 2. Detection of PFAS Mixtures by Ion Transfer DPV

mixture of the two substances				
substance 1	E_{p1}/V	substance 2	E_{p2}/V	detection of individual substances
PFOA	0.22	PFOS	0.32	yes
PFOA	0.22	PFHxS	0.31	yes
PFBS	0.25	PFHxS	0.31	yes
PFBS	0.25	PFOS	0.32	yes
PFOA	0.22	PFBS	0.25	no
PFHxS	0.31	PFOS	0.32	no

CONCLUSIONS

Four per- and polyfluoroalkyl substances (PFOA, PFBS, PFHxS, and PFOS) were studied by ion transfer voltammetry at the μITIES formed at the tips of micropipettes. All these PFAS substances gave well-defined sigmoidal voltammetric waves for transfers from the aqueous to organic phase, indicating radial diffusion of the analytes from the outer aqueous phase to the micrometer-sized interface. On the other hand, a peak shape voltammogram was obtained on the reverse scan, corresponding to linear diffusion of PFAS substances from the in-pipette organic phase to the aqueous phase. The estimated ion-transfer half-wave potentials $E_{1/2}$ for each substance changed according to their lipophilicities, which depends on their structures, including the functional groups present in each substance. Diffusion coefficients of these analytes in the aqueous phase were calculated from the CV data and were in good agreement with the literature values. LODs were in the micromolar to sub-micromolar range. Selectivity for the detection of these four substances in mixtures was investigated. Although their transfer potentials were very close together, most mixtures of two PFAS substances were detectable by DPV. However, PFOA + PFBS and PFHxS + PFOS mixtures produced single peak voltammograms because of the very close proximity of their transfer potentials. Overall, these results show that while ion transfer voltammetry represents a simple strategy for the detection of ionized PFAS, there are limitations in the approach.

ASSOCIATED CONTENT

Supporting Information

The Supporting Information is available free of charge at https://pubs.acs.org/doi/10.1021/acssensors.2c01100.

CV of tetraethylammonium at μITIES; $E_{1/2}$ estimation method; CV of PFAS mixture at μITIES; statistical analysis for DPV detection; and DPV of PFAS mixtures (PDF)

AUTHOR INFORMATION

Corresponding Author

Damien W. M. Arrigan − *School of Molecular and Life Sciences, Curtin University, Perth, WA 6845, Australia;* orcid.org/0000-0002-1053-1273; Email: d.arrigan@curtin.edu.au

Author

Gazi Jahirul Islam − *School of Molecular and Life Sciences, Curtin University, Perth, WA 6845, Australia; Department of Chemistry, University of Barishal, Barisal 8254, Bangladesh*

Complete contact information is available at: https://pubs.acs.org/10.1021/acssensors.2c01100

Notes

The authors declare no competing financial interest.

ACKNOWLEDGMENTS

G.J.I. gratefully acknowledges the award of an Australian Government Research Training Program Scholarship.

REFERENCES

(1) Lau, C., Perfluorinated compounds. In *Molecular, clinical and environmental toxicology*; Springer: 2012; 47−86.
(2) Liu, S.; Yang, R.; Yin, N.; Faiola, F. The short-chain perfluorinated compounds PFBS, PFHxS, PFBA and PFHxA, disrupt human mesenchymal stem cell self-renewal and adipogenic differentiation. *J. Environ. Sci.* **2020**, *88*, 187−199.
(3) Lewandowski, G.; Meissner, E.; Milchert, E. Special applications of fluorinated organic compounds. *J. Hazard. Mater.* **2006**, *136*, 385−391.
(4) Moody, C. A.; Martin, J. W.; Kwan, W. C.; Muir, D. C. G.; Mabury, S. A. Monitoring perfluorinated surfactants in biota and surface water samples following an accidental release of fire-fighting foam into Etobicoke Creek. *Environ. Sci. Technol.* **2002**, *36*, 545−551.
(5) Lehmler, H.-J. Synthesis of environmentally relevant fluorinated surfactants—a review. *Chemosphere* **2005**, *58*, 1471−1496.
(6) Prevedouros, K.; Cousins, I. T.; Buck, R. C.; Korzeniowski, S. H. Sources, Fate and Transport of Perfluorocarboxylates. *Environ. Sci. Technol.* **2006**, *40*, 32−44.
(7) Fair, P. A.; Wolf, B.; White, N. D.; Arnott, S. A.; Kannan, K.; Karthikraj, R.; Vena, J. E. Perfluoroalkyl substances (PFASs) in edible fish species from Charleston Harbor and tributaries, South Carolina, United States: Exposure and risk assessment. *Environ. Res.* **2019**, *171*, 266−277.
(8) Jeong, Y.-J.; Bang, S.; Kim, J.; Chun, S.-H.; Choi, S.; Kim, J.; Chung, M.-S.; Kang, G. J.; Kang, Y.-W.; Kim, J.; Kho, Y.; Joo, Y.; Lee, K. W. Comparing levels of perfluorinated compounds in processed marine products. *Food Chem. Toxicol.* **2019**, *126*, 199−210.

(9) Huang, M. C.; Dzierlenga, A. L.; Robinson, V. G.; Waidyanatha, S.; DeVito, M. J.; Eifrid, M. A.; Granville, C. A.; Gibbs, S. T.; Blystone, C. R. Toxicokinetics of perfluorobutane sulfonate (PFBS), perfluorohexane-1-sulphonic acid (PFHxS), and perfluorooctane sulfonic acid (PFOS) in male and female Hsd:Sprague Dawley SD rats after intravenous and gavage administration. *Toxicol. Rep.* **2019**, *6*, 645−655.
(10) Buck, R. C., Toxicology data for alternative "short-chain" fluorinated substances. In *Toxicological Effects of Perfluoroalkyl and Polyfluoroalkyl Substances*; Springer: 2015; 451−477.
(11) Marchetti, N.; Guzzinati, R.; Catani, M.; Massi, A.; Pasti, L.; Cavazzini, A. New insights into perfluorinated adsorbents for analytical and bioanalytical applications. *Anal. Bioanal. Chem.* **2015**, *407*, 17−21.
(12) Barton, C. A.; Botelho, M. A.; Kaiser, M. A. Solid vapor pressure and enthalpy of sublimation for perfluorooctanoic acid. *J. Chem. Eng. Data* **2008**, *53*, 939−941.
(13) Lau, C.; Butenhoff, J. L.; Rogers, J. M. The developmental toxicity of perfluoroalkyl acids and their derivatives. *Toxicol. Appl. Pharmacol.* **2004**, *198*, 231−241.
(14) Lau, C.; Anitole, K.; Hodes, C.; Lai, D.; Pfahles-Hutchens, A.; Seed, J. Perfluoroalkyl acids: a review of monitoring and toxicological findings. *Toxicol. Sci.* **2007**, *99*, 366−394.
(15) White, S. S.; Calafat, A. M.; Kuklenyik, Z.; Villanueva, L.; Zehr, R. D.; Helfant, L.; Strynar, M. J.; Lindstrom, A. B.; Thibodeaux, J. R.; Wood, C.; Fenton, S. E. Gestational PFOA exposure of mice is associated with altered mammary gland development in dams and female offspring. *Toxicol. Sci.* **2007**, *96*, 133−144.
(16) Upham, B. L.; Park, J.-S.; Babica, P.; Sovadinova, I.; Rummel, A. M.; Trosko, J. E.; Hirose, A.; Hasegawa, R.; Kanno, J.; Sai, K., *Structure-activity−dependent regulation of cell communication by perfluorinated fatty acids using in vivo and in vitro model systems*; National Institute of Environmental Health Sciences: 2009.
(17) Scott, B. F.; Moody, C. A.; Spencer, C.; Small, J. M.; Muir, D. C. G.; Mabury, S. A. Analysis for perfluorocarboxylic acids/anions in surface waters and precipitation using GC−MS and analysis of PFOA from large-volume samples. *Environ. Sci. Technol.* **2006**, *40*, 6405−6410.
(18) Xiao, F.; Sasi, P. C.; Yao, B.; Kubátová, A.; Golovko, S. A.; Golovko, M. Y.; Soli, D. Thermal Decomposition of PFAS: Response to Comment on "Thermal Stability and Decomposition of Perfluoroalkyl Substances on Spent Granular Activated Carbon". *Environ. Sci. Technol. Lett.* **2021**, *8*, 364−365.
(19) Takino, M.; Daishima, S.; Nakahara, T. Determination of perfluorooctane sulfonate in river water by liquid chromatography/atmospheric pressure photoionization mass spectrometry by automated on-line extraction using turbulent flow chromatography. *Rapid Commun. Mass Spectrom.* **2003**, *17*, 383−390.
(20) Surma, M.; Piskuła, M.; Wiczkowski, W.; Zieliński, H. The perfluoroalkyl carboxylic acids (PFCAs) and perfluoroalkane sulfonates (PFSAs) contamination level in spices. *Eur. Food Res. Technol.* **2017**, *243*, 297−307.
(21) Tang, C.; Tan, J.; Wang, C.; Peng, X. Determination of perfluorooctanoic acid and perfluorooctane sulfonate in cooking oil and pig adipose tissue using reversed-phase liquid−liquid extraction followed by high performance liquid chromatography tandem mass spectrometry. *J. Chromatogr. A* **2014**, *1341*, 50−56.
(22) Poothong, S.; Boontanon, S. K.; Boontanon, N. Determination of perfluorooctane sulfonate and perfluorooctanoic acid in food packaging using liquid chromatography coupled with tandem mass spectrometry. *J. Hazard. Mater.* **2012**, *205-206*, 139−143.
(23) Giusto, P.; Lova, P.; Manfredi, G.; Gazzo, S.; Srinivasan, P.; Radice, S.; Comoretto, D. Colorimetric detection of perfluorinated compounds by all-polymer photonic transducers. *ACS Omega* **2018**, *3*, 7517−7522.
(24) Cennamo, N.; D'Agostino, G.; Sequeira, F.; Mattiello, F.; Porto, G.; Biasiolo, A.; Nogueira, R.; Bilro, L.; Zeni, L. A simple and low-cost optical fiber intensity-based configuration for perfluorinated compounds in water solution. *Sensors* **2018**, *18*, 3009.
(25) Takayanagi, T.; Yamashita, H.; Motomizu, S.; Musijowski, J.; Trojanowicz, M. Preconcentration and decomposition of perfluorinated carboxylic acids on an activated charcoal cartridge with sodium biphenyl reagent and its determination at μg L− 1 level on the basis of flow injection-fluorimetric detection of fluoride ion. *Talanta* **2008**, *74*, 1224−1230.
(26) Hemida, M.; Ghiasvand, A.; Gupta, V.; Coates, L. J.; Gooley, A. A.; Wirth, H.-J. R.; Haddad, P. R.; Paull, B. Small-Footprint, Field-Deployable LC/MS System for On-Site Analysis of Per-and Polyfluoroalkyl Substances in Soil. *Anal. Chem.* **2021**, *93*, 12032−12040.
(27) Poma, A.; Turner, A. P. F.; Piletsky, S. A. Advances in the manufacture of MIP nanoparticles. *Trends Biotechnol.* **2010**, *28*, 629−637.
(28) Lahcen, A. A.; Amine, A. Recent advances in electrochemical sensors based on molecularly imprinted polymers and nanomaterials. *Electroanalysis* **2019**, *31*, 188−201.
(29) Fang, C.; Chen, Z.; Megharaj, M.; Naidu, R. Potentiometric detection of AFFFs based on MIP. *Environ. Technol. Innov.* **2016**, *5*, 52−59.
(30) Karimian, N.; Stortini, A. M.; Moretto, L. M.; Costantino, C.; Bogialli, S.; Ugo, P. Electrochemosensor for trace analysis of perfluorooctanesulfonate in water based on a molecularly imprinted poly (o-phenylenediamine) polymer. *ACS Sens.* **2018**, *3*, 1291−1298.
(31) Lu, D.; Zhu, D. Z.; Gan, H.; Yao, Z.; Luo, J.; Yu, S.; Kurup, P. An ultra-sensitive molecularly imprinted polymer (MIP) and gold nanostars (AuNS) modified voltammetric sensor for facile detection of perfluorooctance sulfonate (PFOS) in drinking water. *Sens. Actuators B Chem.* **2022**, *352*, No. 131055.
(32) Kazemi, R.; Potts, E. I.; Dick, J. E. Quantifying Interferent Effects on Molecularly Imprinted Polymer Sensors for Per-and Polyfluoroalkyl Substances (PFAS). *Anal. Chem.* **2020**, *92*, 10597−10605.
(33) Glasscott, M. W.; Vannoy, K. J.; Kazemi, R.; Verber, M. D.; Dick, J. E. μ-MIP: Molecularly Imprinted Polymer-Modified Microelectrodes for the Ultrasensitive Quantification of GenX (HFPO-DA) in River Water. *Environ. Sci. Technol. Lett.* **2020**, *7*, 489−495.
(34) Clark, R. B.; Dick, J. E. Electrochemical Sensing of Perfluorooctanesulfonate (PFOS) Using Ambient Oxygen in River Water. *ACS Sens.* **2020**, *5*, 3591−3598.
(35) Clark, R. B.; Dick, J. E. Towards deployable electrochemical sensors for per-and polyfluoroalkyl substances (PFAS). *Chem. Commun.* **2021**, *57*, 8121−8130.
(36) Hossain, M. M.; Faisal, S. N.; Kim, C. S.; Cha, H. J.; Nam, S. C.; Lee, H. J. Amperometric proton selective strip-sensors with a microelliptic liquid/gel interface for organophosphate neurotoxins. *Electrochem. Commun.* **2011**, *13*, 611−614.
(37) Arrigan, D. W. M. Bioanalytical detection based on electrochemistry at interfaces between immiscible liquids. *Anal. Lett.* **2008**, *41*, 3233−3252.
(38) Arrigan, D. W. M.; Herzog, G.; Scanlon, M. D.; Strutwolf, J., Bioanalytical applications of electrochemistry at liquid-liquid microinterfaces. In *Electroanalytical Chemistry: A Series of Advances: Volume 25*; CRC Press: 2013; 105−178.
(39) Amemiya, S.; Wang, Y.; Mirkin, M. V. Nanoelectrochemistry at the liquid/liquid interfaces. *Specialist periodical reports in electrochemistry* 2013, *12*, 1.
(40) Jing, P.; Rodgers, P. J.; Amemiya, S. High lipophilicity of perfluoroalkyl carboxylate and sulfonate: implications for their membrane permeability. *J. Am. Chem. Soc.* **2009**, *131*, 2290−2296.
(41) Garada, M. B.; Kabagambe, B.; Kim, Y.; Amemiya, S. Ion-transfer voltammetry of perfluoroalkanesulfonates and perfluoroalkanecarboxylates: picomolar detection limit and high lipophilicity. *Anal. Chem.* **2014**, *86*, 11230−11237.
(42) Viada, B. N.; Yudi, L. M.; Arrigan, D. W. M. Detection of perfluorooctane sulfonate by ion-transfer stripping voltammetry at an array of microinterfaces between two immiscible electrolyte solutions. *Analyst* **2020**, *145*, 5776−5786.

https://doi.org/10.1021/acssensors.2c01100
ACS Sens. 2022, 7, 2960−2967

(43) Lee, H. J.; Beattie, P. D.; Seddon, B. J.; Osborne, M. D.; Girault, H. H. Amperometric ion sensors based on laser-patterned composite polymer membranes. *J. Electroanal. Chem.* **1997**, *440*, 73−82.
(44) Goss, K.-U. The pKa values of PFOA and other highly fluorinated carboxylic acids. *Environ. Sci. Technol.* **2008**, *42*, 456−458.
(45) Moroi, Y.; Yano, H.; Shibata, O.; Yonemitsu, T. Determination of acidity constants of perfluoroalkanoic acids. *Bull. Chem. Soc. Jpn.* **2001**, *74*, 667−672.
(46) Taylor, G.; Girault, H. H. J. Ion transfer reactions across a liquid—liquid interface supported on a micropipette tip. *J. Electroanal. Chem. Interfacial Electrochem.* **1986**, *208*, 179−183.
(47) Saito, Y. A theoretical study on the diffusion current at the stationary electrodes of circular and narrow band types. *Rev. Polarogr.* **1968**, *15*, 177−187.
(48) Randles, J. E. A cathode ray polarograph. Part II.—The current-voltage curves. *Trans. Faraday Soc.* **1948**, *44*, 327−338.
(49) Scanlon, M. D.; Strutwolf, J.; Arrigan, D. W. M. Voltammetric behaviour of biological macromolecules at arrays of aqueous| organogel micro-interfaces. *Phys. Chem. Chem. Phys.* **2010**, *12*, 10040−10047.
(50) Beattie, P. D.; Delay, A.; Girault, H. H. Investigation of the kinetics of assisted potassium ion transfer by dibenzo-18-crown-6 at the micro-ITIES by means of steady-state voltammetry. *J. Electroanal. Chem.* **1995**, *380*, 167−175.
(51) Schaefer, C. E.; Drennan, D. M.; Tran, D. N.; Garcia, R.; Christie, E.; Higgins, C. P.; Field, J. A. Measurement of aqueous diffusivities for perfluoroalkyl acids. *J. Environ. Eng.* **2019**, *145*, 06019006.
(52) Kihara, S.; Suzuki, M.; Sugiyama, M.; Matsui, M. The transfer of carboxylate and sulphonate anions at the aqueous/organic solution interface studied by polarography with the electrolyte solution dropping electrode. *J. Electroanal. Chem. Interfacial Electrochem.* **1988**, *249*, 109−122.
(53) Bard, A. J.; Faulkner, L. R., Fundamentals and applications. *Electrochemical Methods* 2001, 2nd edition, 580−632.

https://doi.org/10.1021/acssensors.2c01100
ACS Sens. 2022, 7, 2960−2967